Problems of Stator Flux Estimation in DTC of PMSM Drives

M. Kadjoudj†, N. Goléa* and M.E.H Benbouzid**

Abstract – The DTC of voltage source inverter-fed PMSMs is based on hysteresis controllers of torque and flux. It has several advantages, namely, elimination of the mandatory rotor position sensor, less computation time, and rapid torque response. In addition, the stator resistance is the only parameter, which should be known, and no reference frame transformation is required. The DTC theory has achieved great success in the control of induction motors. However, for the control of PMSM drives proposed a few years ago, there are many basic theoretical problems that must be clarified. This paper describes an investigation into the effect of the zero voltage space vectors in the DTC system and points out that if using it rationally, not only can the DTC of the PMSM drive be driven successfully, but torque and flux ripples are reduced and overall performance of the system is improved. The implementation of DTC in PMSM drives is described and the switching tables specific for an interior PMSM are derived. The conventional eight voltage-vector switching table, which is namely used in the DTC of induction motors does not seem to regulate the torque and stator flux in a PMSM well when the motor operates at low speed. Modelling and simulation studies have both revealed that a six voltage-vector switching table is more appropriate for PMSM drives at low speed. In addition, the sources of difficulties, namely, the error in the detection of the initial rotor position, the variation of stator resistance, and the offsets in measurements are analysed and discussed.

Keywords : DTC, Flux estimation, Offset in measurement, PMSM, Switching tables

1. Introduction

The direct torque control technique possesses advantages such as less parameter dependency and fast torque response when compared to the conventional torque control via pulse width modulation (PWM) current control. In fact, this approach proposes a control scheme where the electromagnetic torque and flux magnitude are estimated with only stator voltages and currents.

PMSMs are widely used in high performance applications such as machines tools, robotics, and motion control because of their high power density, high torque to inertia ratio, and free maintenance. The DTC is a typical example of these applications. Many PMSM drives use an open loop form of torque control, based on the assumption that output torque is proportional to applied current. This assumption may not always be correct due to non-uniformity of magnetic materials, current sensors non-linearities, and current controller limitations. Theses factors can lead to high values of torque ripple and copper loss [1, 2].

In the existing literature, many algorithms have been suggested for the DTC control. The eight voltage-vector switching scheme seems to be suitable only for high speed operation of the motor while at low speed the six voltage-vector switching scheme, avoiding the two zero voltage-vectors, seems to be appropriate for the permanent magnet synchronous motor drive.

The voltage vector strategy using switching table is widely researched and commercialized, because it is very simple in concept and very easy to be implemented. The control block diagram of the proposed method is shown in Fig. 1. The stator fluxes linkages are calculated from stator voltages and currents [3, 4]. The DTC is increasingly drawing interest because of,

- Simplicity of its structure.
- Elimination of the current controllers.
- Inherent delays.
- Elimination of rotor position sensor.

Although the direct torque control has attractive features such as fast dynamic response and low parameter dependence, there is a problem of a drift in stator flux estimation. In direct torque control, the stator flux is estimated by integrating the difference between the input voltage and the voltage drop across the stator resistance,

$$\phi_{s\alpha} = \int (V_{s\alpha} - R_s . I_{s\alpha}) dt$$
$$\phi_{s\beta} = \int (V_{s\beta} - R_s . I_{s\beta}) dt \quad (1)$$

† Corresponding Author:Dept. of Electrical Engineering, University of Batna, Algeria (kadjoudj_m@yahoo.fr)
* Dept. of Electrical Engineering, University of Oum El Bouaghi, Algeria
** IUT Brest, Dept. GEII, University of Western Brittany, France
Received 25 October 2006 ; Accepted 5 June 2007

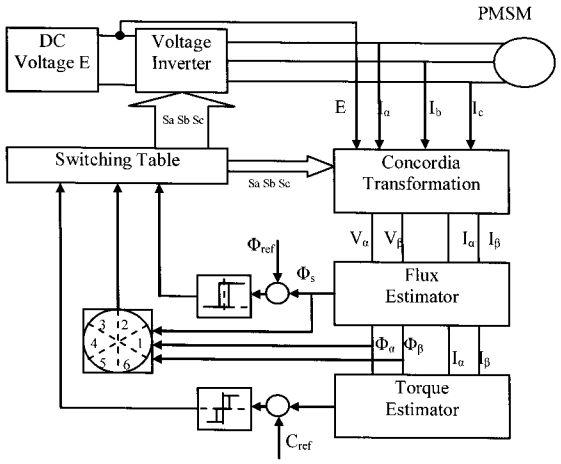

Fig. 1. DTC block diagram of PMSM

and then

$$\phi_s = \sqrt{\phi_{s\alpha}^2 + \phi_{s\beta}^2}$$
$$\angle\theta_s = \tan^{-1}(\phi_{s\beta} / \phi_{s\alpha}) \quad (2)$$

This paper investigates the problem of the offset error in estimating stator flux linkage and torque for DTC controlled PMSM drives.

When the stator flux is indirectly estimated from the integration of the back emf, any DC offset is also integrated and would eventually lead to a large drift in the stator flux linkage. These sensors have temperature dependent dc-offset. Since the current measurement path contains analog devices, dc-offset is an inevitable problem.

The model suffers from several problems. Firstly, the measured signals of the inverter DC-link voltage and motor phase currents suffer from the offsets which in turn result in inaccuracies of the stator flux linkage and torque. Secondly, the variation of the stator resistance due to change in temperature and stator input frequency also contribute in the error, especially at low speed when the voltage drop may become significant compared to the amplitude of the voltage input. This error manifests itself in producing large errors in the computation of the stator flux estimation [5, 6].

2. Machine Equations

The motor considered in this paper is an interior PMSM that consists of a three phase stator winding and a PM rotor. The voltage equations in a synchronous reference frame can be derived as follows [3-6],

$$V_d = R_s.I_d. + \frac{d\phi_d}{dt} - \omega_r.\phi_q \quad (3)$$

$$V_q = R_s.I_q. + \frac{d\phi_q}{dt} + \omega_r.\phi_d \quad (4)$$

Where the direct and inverse axes flux linkages are,

$$\phi_d = L_d.I_d. + \phi_f \quad (5)$$

$$\phi_q = L_q.I_q \quad (6)$$

The electromagnetic torque of the motor can be evaluated as follows,

$$C = \frac{3}{2} n_p.\{\phi_f.I_q + (L_d - L_q).I_d.I_q\} \quad (7)$$

The motor dynamics can be simply described by Equation (8).

$$\frac{J}{n_p}\frac{d\omega_r}{dt} + \frac{f}{n_p}.\omega_r = C_{em} - C_{st} \quad (8)$$

By using the concept of the field orientation, it can be assumed that the d-axis current is controlled to be zero. Thus, the PMSM has the best dynamic performance and also operates in the most efficient state. Under this assumption, the contribution of the second term of the electric torque equation becomes effectively negligible and the reduced dynamic model of the PMSM is given by the following equations,

$$\frac{dI_q}{dt} = \frac{1}{L_q}.V_q - \frac{R_s}{L_q}.I_q - \frac{\phi_f}{L_q}.\omega_r$$
$$\frac{J}{n_p}\frac{d\omega_r}{dt} = K_T.I_q - \frac{f}{n_p}.\omega_r - C_{st} \quad (9)$$
$$\frac{d\theta}{dt} = \omega_r$$

3. DTC Algorithm

The electromagnetic torque equation can be expressed in terms of the stator flux linkage and its angle with respect to the rotor flux linkage as follows,

$$C = 0.75 n_p\left[\frac{2.\phi_f.\phi_s}{L_d}.\sin(\delta) + \phi_s^2.\left\{\frac{1}{L_q} - \frac{1}{L_d}\right\}.\sin(2\delta)\right] \quad (10)$$

For a surface magnet motor, Equation (10) becomes,

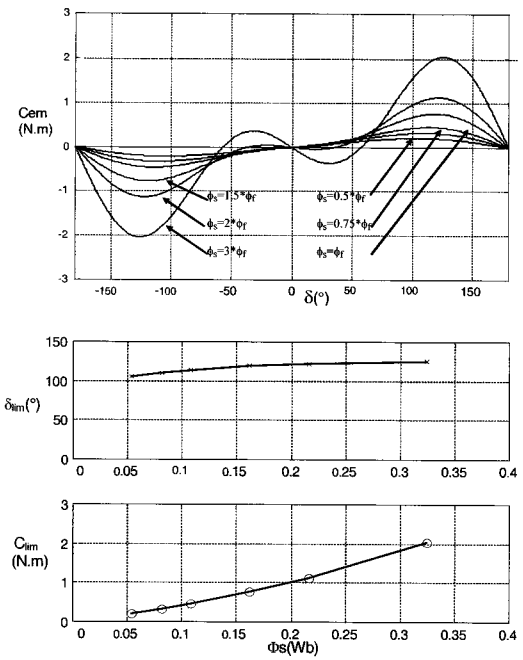

Fig. 2. Torque – angle characteristics of PMSM

$$C = 1.5.n_p.\frac{\phi_f.\phi_s}{L}.\sin(\delta) \qquad (11)$$

The angle between the stator and rotor flux linkages, noted δ, is the load angle when the stator resistance is neglected. In the steady state, the load angle is constant corresponding to a load torque. Both the stator and rotor fluxes rotate at synchronous speed. In transient state, the load angle varies and the flux vectors rotate at different speeds. The relationship between torque C and δ may be linear in some cases, and may not be linear in others cases as depicted by Fig. 2. The limiting δ_{lim} and C_{lim} for various levels of stator flux linkage ϕ_s must also be adhered to.

Fig. 2 presents the torque-load angle characteristics of the PMSM drive when the flux amplitude is at $0.5\phi_f$, $0.75\phi_f$, ϕ_f, $1.5\phi_f$, $2\phi_f$, and $3\phi_f$. For the two last cases, the derivative of torque near zero crossing is negative. Then, the DTC cannot be applied. The condition for positive derivative of the torque with respect to the load angle is given by Equation (12). For obtaining fast dynamic torque response, the amplitude of stator flux linkage should be chosen according to relation (12).

$$\phi_s < \frac{L_q}{L_q - L_d}.\phi_f \qquad (12)$$

The derivative of torque in Equation (10) is positive if, $-\pi/2<\delta<\pi/2$. Then, the increase of torque is proportional to the increase of the angular velocity δ. In other words, the

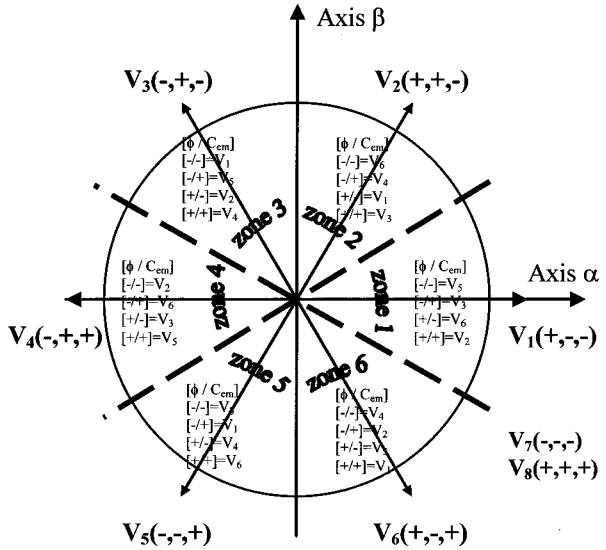

Fig. 3. Sectors and voltage vectors

stator flux ϕ_s should be controlled in such a way that the amplitude is kept constant and the rotating speed is controlled as fast possible to obtain the maximum change in actual torque. There are six non-zero voltage vectors V_1-V_6 and two zero voltage vectors V_7-V_0.

- $V_1(1\ -1\ -1) \Rightarrow S_a=1\ ;\ S_b=-1\ ;\ S_c=-1.$
- $V_2(1\ 1\ -1)) \Rightarrow S_a=1\ ;\ S_b=1\ ;\ S_c=-1.$
- $V_3(-1\ 1\ -1) \Rightarrow S_a=-1; S_b=1; S_c=-1$
- $V_4(-1\ 1\ 1) \Rightarrow S_a=-1\ ;\ S_b=1\ ;\ S_c=1$
- $V_5(-1\ -1\ 1) \Rightarrow S_a=-1\ ;\ S_b=-1\ ;\ S_c=1$
- $V_6(1\ -1\ 1) \Rightarrow S_a=1\ ;\ S_b=-1\ ;\ S_c=1$
- $V_7(-1\ -1\ -1) \Rightarrow S_a=-1;\ S_b=-1,\ S_c=-1$
- $V_8(1\ 1\ 1) \Rightarrow S_a=1; S_b=1,\ S_c=1$

The two zero voltage vectors are at the origin and the six non-zero voltage vectors are 60° apart from each other in the voltage vector plane as depicted by Fig. 3.

During the switching intervals, each applied voltage vector remains constant and the stator fluxes linkages are given in the stationary reference frame as,

$$\phi_\alpha(k+1) = \phi_\alpha(k) + h\left[V_\alpha(k) - R_s.I_\alpha(k)\right] \qquad (13)$$

$$\phi_\beta(k+1) = \phi_\beta(k) + h\left[V_\beta(k) - R_s.I_\beta(k)\right] \qquad (14)$$

Neglecting the stator resistance, Equations 13 and 14 imply that the tip of the stator vector will move in the direction of the applied voltage vector in a straight line as indicated in Fig. 4. For controlling the amplitude of the stator flux, the voltage vector plane is divided into six regions. Each of these regions is 60° wide. In each region, two adjacent voltage vectors may be selected to increase or decrease the stator flux amplitude and give a minimum switching frequency [7].

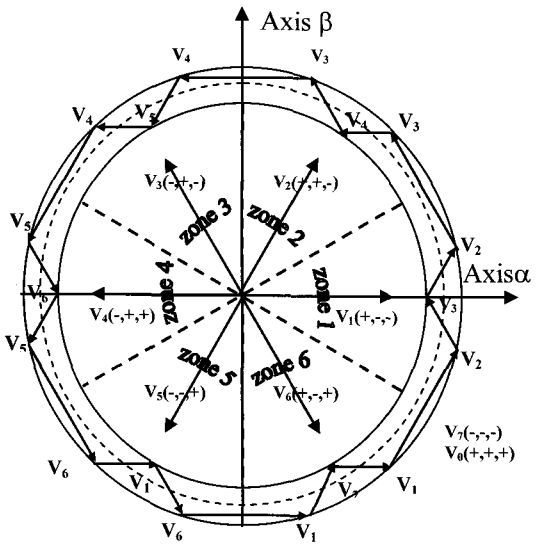

Fig. 4. Control of stator flux linkage with selected stator voltage vectors.

The six-region control is distinguished based on the inequalities:

$$-\frac{\pi}{6}+(1-N).\frac{\pi}{3} \le \theta(N) < \frac{\pi}{6}-(1-N).\frac{\pi}{3} \qquad (15)$$

In Fig. 4, the space between the two circles represents the hysteresis band in stator flux linkage amplitude which in turn is equal to the rated flux when operation below the based speed is called for. For field weakening, these two circles contract inward.

4. Problem of the Voltage Switching Tables

The torque and flux hysteresis controllers select the appropriate voltage vectors. Tables 1 and 2 indicate the six and eight voltage vector switching strategies, in each region C and ϕ are increasing or decreasing functions of time. From Table 1, the torque and flux are increased or decreased by selecting only the six non-zero voltage vectors. The torque is changed by reversing the movement of the stator flux vector at each state of the hysteresis controller output.

Table 1. The six voltage vectors switching table

		Z=1	Z=2	Z=3	Z=4	Z=5	Z=6
R_ϕ=1 ($\phi\uparrow$)	R_c=1 (C↑)	V_2	V_3	V_4	V_5	V_6	V_1
	R_c=0 (C↓)	V_6	V_1	V_2	V_3	V_4	V_5
R_ϕ=0 ($\phi\downarrow$)	R_c=1 (C↑)	V_3	V_4	V_5	V_6	V_1	V_2
	R_c=0 (C↓)	V_5	V_6	V_1	V_2	V_3	V_4

Table 2. The eight classic voltage vectors switching table

		Z=1	Z=2	Z=3	Z=4	Z=5	Z=6
R_ϕ=1 ($\phi\uparrow$)	R_c=1(C↑)	V_2	V_3	V_4	V_5	V_6	V_1
	R_c=0(C↓)	V_7	V_0	V_7	V_0	V_7	V_0
R_ϕ=0 ($\phi\downarrow$)	R_c=1(C↑)	V_3	V_4	V_5	V_6	V_1	V_2
	R_c=0(C↓)	V_0	V_7	V_0	V_7	V_0	V_7

From Table 2, it is clear that when the torque is increasing or decreasing, the flux linkage can be increased or decreased by selecting alternatively one of the six non-zero voltage vectors and one of the two zero voltage vectors.

Use of the six voltage vectors switching table implies that the stator flux linkage is always kept in motion, making it go forward and backward in order to regulate the torque loop. For controlling the amplitude of stator flux and therefore for changing the torque, zero voltage vectors V_7 and $V_8$are not used in PMSM drives.

In Tables 1 and 2, R_ϕ and R_C are the outputs of the hysteresis controllers. Z=1,...6 represent the region's numbers for the stator flux linkage positions.

To study the performance of the DTC control, the simulation of the system was conducted using a Matlab programming environment. Fig. 5 shows that the motor can follow the command torque very well. However, relatively high torque ripples are observed. The estimated stator flux has the same form of the flux reference. Fig. 5 indicates how the voltage vectors are selected for keeping ϕ_s within the hysteresis band when ϕ_s is rotating in the counter-clockwise direction.

The PMSM was simulated under the DTC drive system at high and low speed. Fig. 6 reveals loss of control over torque and stator flux when the zero voltage algorithm is used. These could not be attributed to factors such as offsets in the measurements of motor terminal quantities and the variation of stator resistance which are known

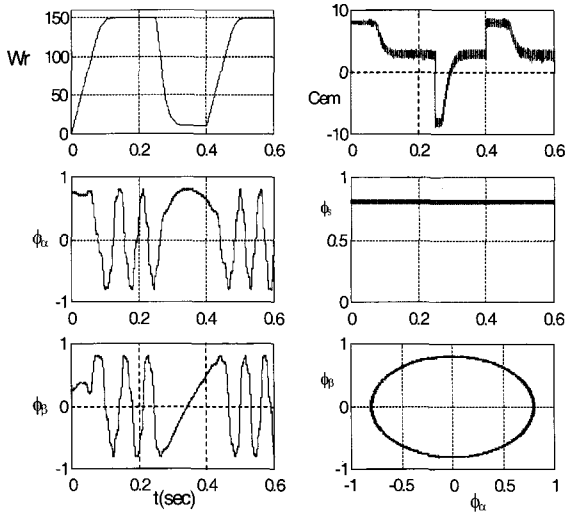

Fig. 5. DTC without zero-voltage vectors

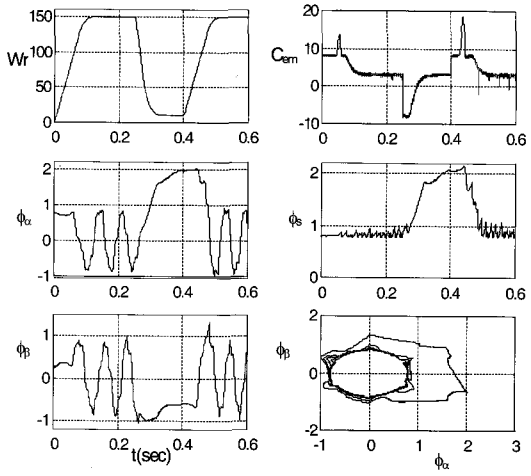

Fig. 6. DTC with zero voltage vectors

sources of problems in DTC. It is seen however, that the ripples in torque and flux characteristics are considerably lower when the eight voltage vectors in Table 2 are used. This implies that Table 2 is more appropriate for high speed operations [8].

As mentioned from Equation (10), the torque is proportional to the angle δ, which must be changed quickly. Unlike the asynchronous motor where change of slip frequency is brought about by applying zero voltage vectors, the angle δ in the case of PMSM is determined also by the position of the rotor flux linkage which is non zero at all times. To control torque at low speed, quick change of δ can be obtained by avoiding the zero voltage vectors and by applying vectors that move the stator flux relative to rotor flux as quickly as possible. At high speed, this may not be necessary where the rotor moves sufficiently to produce the required change in torque. The conventional eight voltage vector switching table is normally used in the DTC of induction motors and does not seem to regulate the torque and stator flux in PMSM drives well when the motor operates at low speed.

To overcome the previously mentioned difficulties, an algorithm is proposed in Table 3 that consists in combination of advantages of the two classic tables simultaneously and has the benefit of conceptual simplicity. Fig. 7 shows the control structure for selecting the voltage vectors and keeping torque and flux linkage within pre-selected hysteresis bands.

Table 3. Switching table with three level controller

		Z=1	Z=2	Z=3	Z=4	Z=5	Z=6
R_ϕ=1 (φ↑)	R_c=1 (C↑)	V_2	V_3	V_4	V_5	V_6	V_1
	R_c=0	V_7	V_0	V_7	V_0	V_7	V_0
	R_c=-1(C↓)	V_6	V_1	V_2	V_3	V_4	V_5
R_ϕ=0 (φ↓)	R_c=1 (C↑)	V_3	V_4	V_5	V_6	V_1	V_2
	R_c=0	V_0	V_7	V_0	V_7	V_0	V_7
	R_c=-1(C↓)	V_5	V_6	V_1	V_2	V_3	V_4

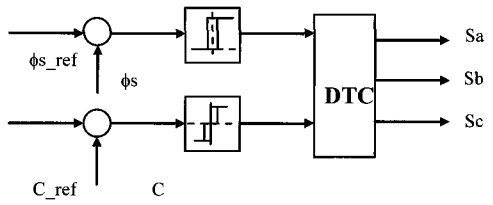

Fig. 7. Torque and flux hysteresis controllers

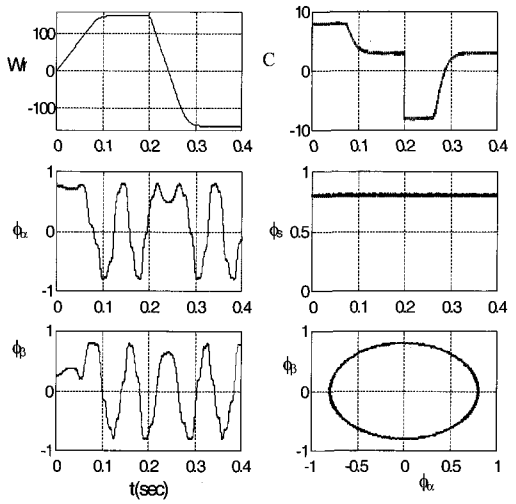

Fig. 8. DTC with three level torque controller

The hysteresis band has to be set large enough to limit the inverter switching frequency below a certain level. The amplitude of the hysteresis band strongly influences the inverter performance such as torque and flux ripples, current harmonics, and switching frequency. Modelling results for similar operating conditions with a three level torque hysteresis controller is depicted in Fig.8.

The switching frequency variation characteristic of the flux hysteresis controller is different from that of the torque hysteresis controller. As presented in Fig. 9 the switching frequency has a maximum value in a medium speed range.

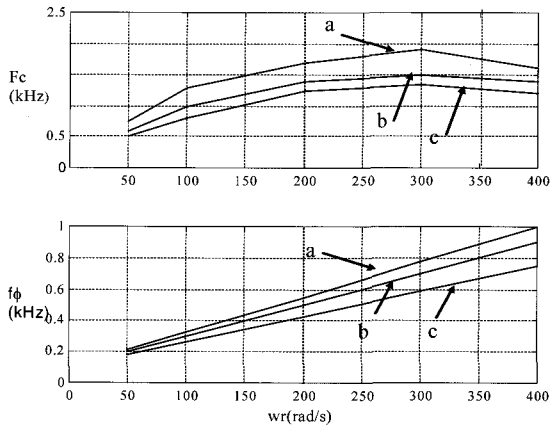

Fig. 9. Switching frequencies of torque and flux versus speed. a)ΔC= Δφ=0.01 b) ΔC= Δφ=0.025 c) ΔC= Δφ=0.1.

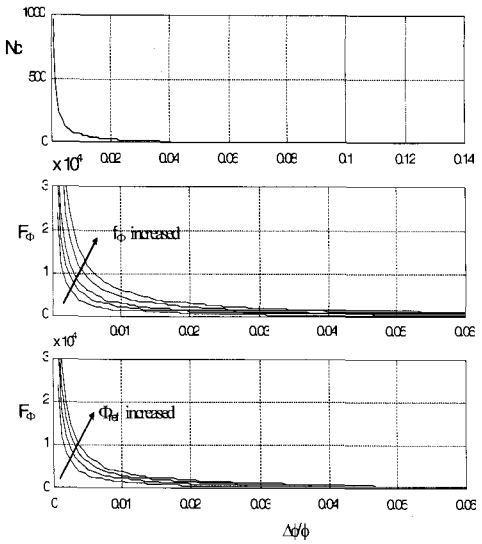

Fig. 10. Flux regulator switching frequency

For the flux controller, the switching frequency is proportional to the motor speed. This phenomenon causes flux and torque controllers to have different contributions to the total switching frequency. It means that the amplitude of flux and torque hysteresis controllers should be regulated separately for effective utilization of given total switching frequency controller command.

The commutation number and stator flux regulator switching frequency are given respectively by [11] and [12],

$$N_c = 0.6.\frac{\phi_{ref}}{\Delta\phi} \tag{16}$$

$$F_\phi = \frac{6.\phi_{ref}.f_{\phi s}}{10.\Delta\phi} \tag{17}$$

Fig. 10 shows that a reduced switching frequency is obtained by increasing the size of the flux hysteresis band. The switching frequency is related linearly to the size window. For low speed, the application of the two zero voltage vectors is dominant and implies a reduced torque

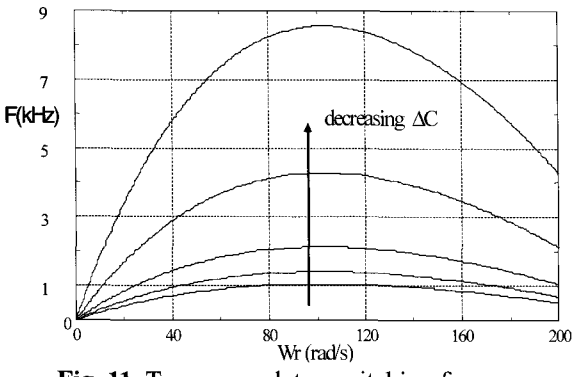

Fig. 11. Torque regulator switching frequency

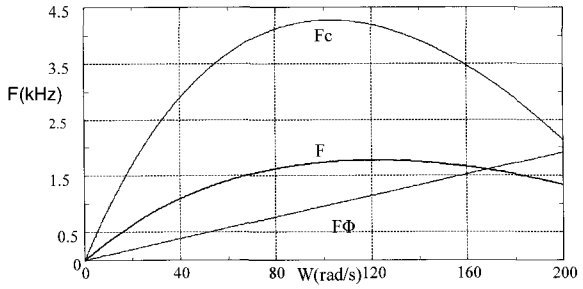

Fig. 12. Total inverter switching frequency

variation. This may be achieved at a lower switching frequency of the inverter.

For the high speeds range, the six non-zero voltage vectors are frequently applied, which causes a lower variation of torque with reduced switching frequency when the motor speed is increased. For medium speeds, high switching frequency is achieved with decreasing the torque size window as it is shown in Fig. 11.

The inverter switching frequency can be approximately derived from the flux and torque regulator frequencies,

$$F = \frac{F_\phi + F_C}{3} \tag{18}$$

Fig. 12 illustrates the total inverter switching frequency which has maximum value in a medium speed range while switching frequency of the flux controller is proportional to the rotating speed [6], [10].

5. Effect of the stator resistance variation

The stator resistance Rs varies mainly due to the change of temperature which, in turn depends on such factors as duty cycle, load, ambient conditions, and speed. Some of these factors are unpredictable. There is also some change due to skin effect which depends on input frequency. The effect of the variation of stator resistance leads to large variation in estimated stator flux linkage. In DTC, the stator flux is estimated using Equation (19), when Φs, Vs and Is represent the stator flux linkage, voltage, and current vectors respectively.

$$\phi_s = \int (V_s - R_s.I_s)dt \tag{19}$$

The variation of Rs may introduce significant errors in the calculation of stator flux and thereby the overall performance of the DTC system. At low speeds, the back electromotive force term is small and the resistive drop is comparable with the supply voltage magnitude. Any change in stator resistance gives erroneous estimation of

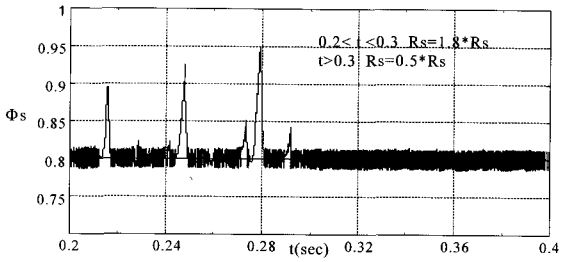

Fig. 13. Effect of stator resistance variation

stator flux and consequently of the electromagnetic torque. An error in the angular position of the stator flux linkage position is also important as it can cause the controller to select an incorrect switching state. Simulation studies indicate that the drive system becomes unstable if the stator resistance value used in the controller is higher than that of the machine actual resistance. Fig. 13 shows that the stator flux linkage exhibits undesired oscillation when Rs is increased. So a mismatch between nominal and actual resistance value can create instability. At high speeds, the stator resistance drop is small compared to the back emf and hence can be neglected [11, 12].

The stator resistance changes due to temperature variations with a large extent and to stator frequency variation with a smaller degree. Such changes deteriorate the drive performance by introducing errors in the estimated magnitude and position of the flux linkage vector. This in turn affects the estimation of the torque, particularly at low speeds [9, 13].

In reality, the stator resistance does not change in step manner. So, the instability result under a step change is not so practical. In actual operating conditions, the rate of change of temperature is very slow and so the stator resistance changes in an unpredictable manner.

6. Effect of the offsets in measurement

The source of offset in measurement is the thermal offset of analog integrators used in signal processing. Offset also arises from DC components that result after a transient change. In reality, the offset is unpredictable and changes with temperature. It may introduce unacceptable drift in the stator flux estimation and then cause an error in torque estimation, so the drive system may become unstable.

The offset error is non-periodical and unidirectional and examined by extensive simulation studies. Fig. 14 indicates the modelling results when offset error is artificially introduced in direct current component. It is seen that the accumulation of the offset error in the current causes the torque oscillation to increase and the stator flux to drift from its origin. The compensation for this drift is possible with a programmable cascaded low pass filter.

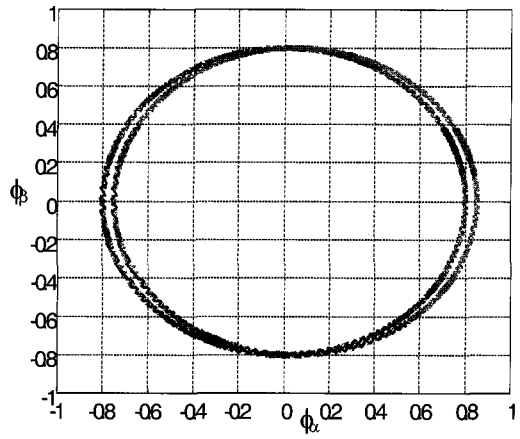

Fig. 14. Effect of the offset in current measurement

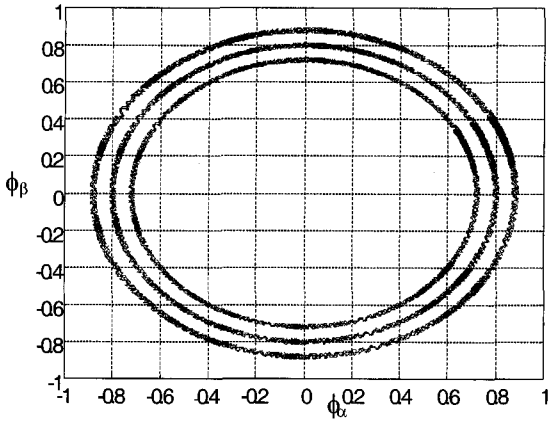

Fig. 15. Effect of the offset in DC voltage measurement

$$\phi_{\alpha.actual} = \phi_{\alpha} - \frac{\sqrt{3}}{2}.R_s.\int I_a.dt \tag{20}$$

$$\phi_{\beta.actual} = \phi_{\beta} - \frac{1}{\sqrt{2}}.R_s.\int (I_b - I_c).dt \tag{21}$$

Offsets in measurement of the DC-link voltage and phase currents are inevitable. They are due to the sensors and the signal conditioning circuits used. The centred circle shows the stator flux linkage when the actual DC link voltage is the nominal value. The inner circle in Fig. 15 depicts the flux linkage when E= 0.9*En and the larger circle represents Φs when E=1.2*En.

$$V_s = \sqrt{\frac{2}{3}}.(E + \Delta E).(S_a + a.S_b + a^2.S_c) \tag{22}$$

7. Effect of the initial flux vector estimation

One of the attractive features of the DTC is that the requirement for the continuous rotor position is eliminated. Only the initial rotor position is needed. Error in the initial flux value is not a significant factor since its effect is only seen when the motor is first started. The integration process

Table 4. Estimation of the initial flux vector

Flux magnitude	Convergence intervals
0.5. ϕ_{ref}	-15° to 138°
0.8. ϕ_{ref}	-28° to 177°
ϕ_{ref}	-17° to 165°
1.2. ϕ_{ref}	-16° to 115°
1.5. ϕ_{ref}	-11° to 100°

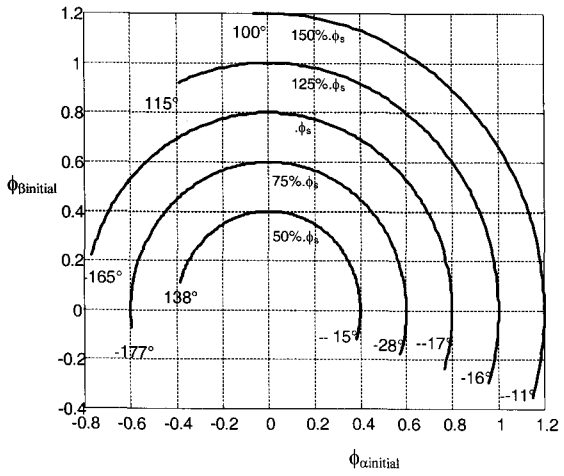

Fig. 16. Upper and lower limits of the initial flux estimation with convergence intervals

in (19), which runs continuously, requires knowledge of the initial stator flux position at start [8, 9].

At start, the stator current is assumed to be zero, so that the flux linkage due to rotor only must be known at the starting condition. Some experimental and modelling studies found that initial flux has to be known only approximately and the error in initial position affects the initial starting transient of the drives [13, 14]. This dithering is unacceptable in some applications such as electric propulsion and high performance servo-systems.

Table 4 and Fig. 16 illustrate the convergence range for the initial flux position. The initial flux position is identified with sufficient accuracy for various levels of the flux magnitude.

In order to evaluate the effects of initial flux vector limit, the outputs are shown together for comparison in Fig. 17 and Fig. 18. It is seen that in the steady state, the fluxes' evolution are exactly the same and the only difference is in the initial transient period.

The flux linkage of Fig. 17, Fig. 18, and 19 are plotted in stator αβ plane. It is seen that the actual trajectory overlapped on the desired trajectory. In all cases, the improved results lead to stable operating conditions with the same value of both amplitude and frequency of the flux components. It should be noted that, considering θs=-17° for the flux magnitude of Φs= Φref, small deviations of the flux trajectories are present and no appreciable differences are observed in the performance of the two flux components.

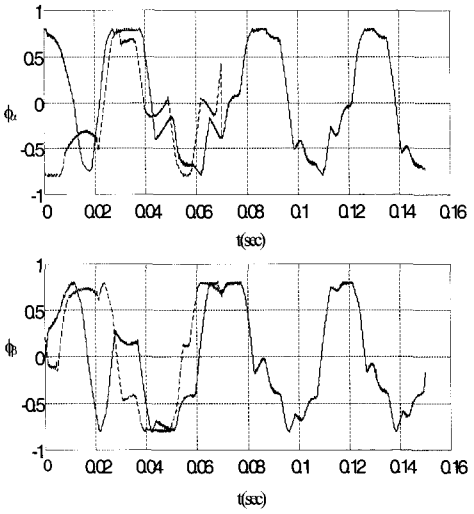

Fig. 17. Flux linkage in αβ plane with upper initial flux position (θs=-17°) for $\phi_{s=}$ 0.8 Wb

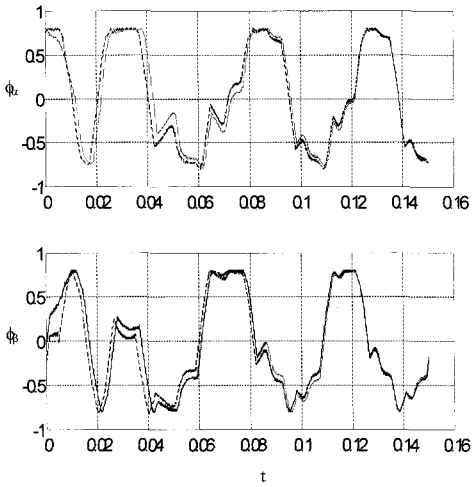

Fig. 18. Flux linkage in αβ plane with lower initial flux position (θs=165°) for $\phi_{s=}$ 0.8Wb.

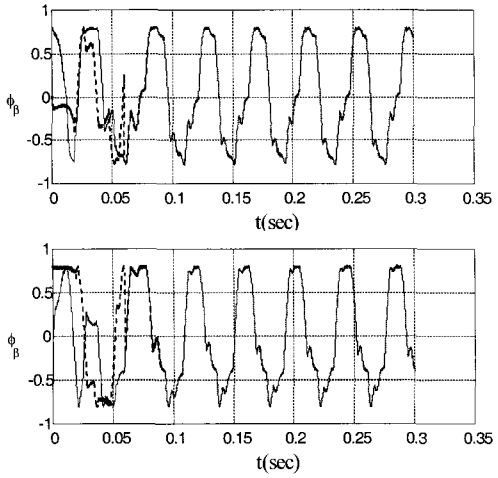

Fig. 19. Flux linkage in αβ plane with θs=90° for $\phi_{s=}$ 0.8Wb.

Since the basic DTC principle is to rotate the flux

linkage forward if the torque must be increased, and reverse if the torque must be decreased, the stability is not guaranteed with the change of stator resistance, large offsets in measurements, and initial flux position error.

8. Conclusion

This paper investigates some of the major problems associated with the DTC of PMSM drives, the offset error in measurement, the stator resistance change, and initial flux value in estimating stator flux linkage and torque for a DTC control.

It is seen that the DTC algorithm is capable of working from low speed to high speed and exhibits very good dynamic and steady state performance. However, the offset error may deteriorate the performance by introducing error in the estimated flux linkage and in turn cause the torque of a motor to oscillate at the stator electrical frequency.

The offsets are DC signals in nature and their magnitudes also depend on temperature. The integration process in the equation of stator flux estimation will integrate these errors and they will grow to large values leading to instability.

The use of a switching table with zero voltage vectors revealed loss of control, which could not be attributed to factors such as offsets in measurement and variation of stator resistance, which are known sources of problems for the DTC. The eight voltage vector switching table is found to be preferable for high speed operating conditions with lower torque and stator flux ripples. The main advantages of the combined structure are,

- Stable and efficient structure.
- Improvement of torque ripple characteristic in a large speed range.
- Fast response and robustness merits entirely preserved.

APPENDIX - RATED DATA OF THE PMSM

Rated values		
Frequency	50 Hz	
Voltage (Δ/Y)	220 V	
Speed 1500 rpm		
Torque 3 N·m		
Pole pair (n_p)	2	
Rated parameters		
ϕf	0.314	Wb
L_d	0.0349	H
L_q	0.0627	H
J	0.003	kg·m^2
f	0.00008	N·m·s
Rs	*1.4 Ω*	

References

[1] A. Llor, B. Allard, X. Lin-Shi, J.M. Rtif, "Comparison of DTC implementations for synchronous machines," 35th annual IEEE power electronics conference, Aachen Germany, pp. 3581-3587, 2004.

[2] M. Kadjoudj, M.E. Benbouzid, C. Ghennai, D.Diallo, "A Robust hybrid current control for PMSM drives," IEEE trans. on energy conversion, vol. 19, No. 1, pp. 109-115, 2004.

[3] J.X. Xu, S.K. Panda, Y.J. Pan, T.H. Lee, B.H. Lam, "A Modular control scheme for PMSM speed control with pulsating torque minimization," IEEE trans. on industrial electronics, vol. 51, No. 3, pp. 526-530, June 2004.

[4] L. Tang, L. Zhong, M. Rahman and Y.Hu, "A Novel direct synchronous machine drive with fixed switching frequency," IEEE trans. on power electronics, vol. 19, No. 2, pp. 262-271, March 2004.

[5] J. Faiz, H.M. Zonoozi, "A Novel technique and control of stator flux of a salient pole PMSM in DTC method based on MTPF," IEEE trans. on industrial electronics, vol. 50 No 2. pp. 262-271, April 2003.

[6] M. Kadjoudj, S. Taibi, N. Golea, M.E. Benbouzid, "Modified DTC of PMSM drives with dither signal injection and nonhysteresis controller," Electromot. Journal, vol. 13, No. 4, pp. 262-270, 2006.

[7] J.K. Kang, S.K. Sul, "New direct torque control of induction motor for minimum torque ripple and constant switching frequency," *IEEE Trans. On ind. Appl.*, vol. 35, No. 5, pp. 1076-1082, 1999.

[8] S.K. Chung and al., "A new instantaneous torque control of PMSM for high performance direct drive applications," *IEEE Trans. Power Electronics*, vol. 13, No. 3, pp. 388-400, 1998.

[9] M.F. Rahman, M.E. Haque, L. Tang, L. Zhong, "Problems associated with the DTC of an interior PMSM drive and their remedies," IEEE trans. on industrial electronics, vol. 51, No. 4, pp. 799-808, August 2004.

[10] C. French, P. Acarnley, "Direct torque control of permanent magnet drives," *IEEE Trans. On ind. Appl.*, vol. 32, no. 5, pp. 1080-1088, 1996.

[11] C. Lascu, I. Boldea, F. Blabjerg, "A modified direct torque control for induction motor sensorless drive," *IEEE Trans. On ind. Appl.*, vol. 36, no. 1, pp. 22-30, 2000.

[12] J.K. Kang, D. Chang, S.K. Sul, "DTC of induction machine with variable amplitude control of flux and torque hysteresis bands," conf. of the *IEEE*, vol. 1, pp. 640-642, 1999.

[13] M. Pacas, J. Weber, "Predictive direct torque control for the PM synchronous machine," IEEE trans. on industrial electronics, vol. 52, No. 5, pp. 1350-1356, October 2005.
[14] J. Luukko, O. Pyrhonen, M. Niemela, J. Pyrhonen, "Limitation of the load angle in a direct torque controlled synchronous machine drive," IEEE trans. on industrial electronics, vol. 51, No. 4, pp. 793-798, August 2004.

Mohamed Kadjoudj
He was born in Batna, Algeria in 1964. He received his B.Sc., M.Sc., and Ph.D. degrees in Electrical Engineering from the University of Batna, Algeria, in 1988, 1992, and 2003, respectively. Currently, he is an Associate Professor at the Electrical Engineering Institute of the University of Batna. His current research interests include electric machines and drive control, power electronics, and intelligent motion control and diagnosis.

Noureddine Goléa
He was born in Batna, Algeria, in 1967. He received his B.Sc. and M.Sc. degrees from Setif University, Algeria, and his Ph.D. from Batna University, Algeria, all in industrial control in 1991, 1994, and 2000, respectively. From 1991 to 1994, he was with the Electronics Institute at Setif University, and from 1994 to 1996, he was with the Electronics Institute at Batna University. Currently, he is a Professor of Electrical Engineering at the Institute of Oum El-Bouaghi University, Algeria. His research interests are nonlinear and adaptive control and intelligent motion control.

Mohamed El Hachemi Benbouzid
(S'92–M'94–SM'98) He was born in Batna, Algeria in 1968. He received his B.Sc. degree in Electrical Engineering from the Electrical Engineering Institute of Batna University, Batna, Algeria, in 1990, and his M.Sc. and Ph.D. degrees in Electrical and Computer Engineering from the National Polytechnic Institute of Grenoble, France, in 1991 and 1994, respectively. In 2000, he received the "*Habilitation à Diriger des Recherches*" degree from the University of Picardie "Jules Verne." Currently, he is Professor of Electrical and Computer Engineering at the Institute of Brest, France. His current research interests include electric machines and drive control and diagnosis.